Identification of Inhibitors of Protein Kinase B Using Fragment-Based Lead Discovery†

Gordon Saxty,‡ Steven J. Woodhead,*,‡ Valerio Berdini,‡ Thomas G. Davies,‡ Marcel L. Verdonk,‡ Paul G. Wyatt,‡ Robert G. Boyle,‡ David Barford,§ Robert Downham,‡ Michelle D. Garrett,|| and Robin A. Carr‡

Astex Therapeutics Ltd., 436 Cambridge Science Park, Milton Road, Cambridge, CB4 0QA, United Kingdom, Section of Structural Biology, Institute of Cancer Research, Chester Beatty Laboratories, 237 Fulham Road, London, SW3 6JB, United Kingdom, and Cancer Research UK Centre for Cancer Therapeutics, The Institute of Cancer Research, 15 Cotswold Road, Sutton, Surrey, SM2 5NG, United Kingdom

Received January 23, 2007

Abstract: Using fragment-based screening techniques, 5-methyl-4-phenyl-1*H*-pyrazole (IC_{50} 80 μM) was identified as a novel, low molecular weight inhibitor of protein kinase B (PKB). Herein we describe the rapid elaboration of highly potent and ligand efficient analogues using a fragment growing approach. Iterative structure-based design was supported by protein−ligand structure determinations using a PKA−PKB "chimera" and a final protein−ligand structure of a lead compound in PKBβ itself.

Protein kinase B (PKB[a] or Akt) is a serine/threonine kinase that plays a central role in the regulation of a variety of signal transduction pathways integral to the control of cell growth, differentiation, and division.[1,2] Disregulation and overexpression of PKB has been demonstrated in a growing number of human malignancies, thus providing a potential mechanism for the survival and progression of tumor cells.[2−6] As such, inhibition of PKB, either as a monotherapy or in combination with other chemotherapeutics, is considered to be a potentially valuable approach to the treatment of cancers. The most exemplified strategy for inhibiting PKB targets the kinase domain by competitive inhibition of the ATP binding site. A number of small molecule inhibitors that exploit this approach have been reported.[7−9]

The recent availability of the three-dimensional crystal structure of active, phosphorylated PKBβ[10] (Akt-2) has enhanced opportunities for the development of novel ATP-competitive inhibitors. However, its application to iterative structure-based design has so far been limited by the lack of a robust, soakable crystal form. Structure-based approaches have therefore predominantly resorted to employing surrogate systems, such as the closely related kinase PKA,[9,11,12] or mutant forms of PKA, in which ATP-site residues are mutated to form a PKA−PKB "chimera".[7] We have, however, recently reported a novel method for obtaining crystal structures of PKBβ itself in complex with ligands,[13] and for the purposes of the research reported in this manuscript, both PKA−PKB and PKBβ crystal structures were used.

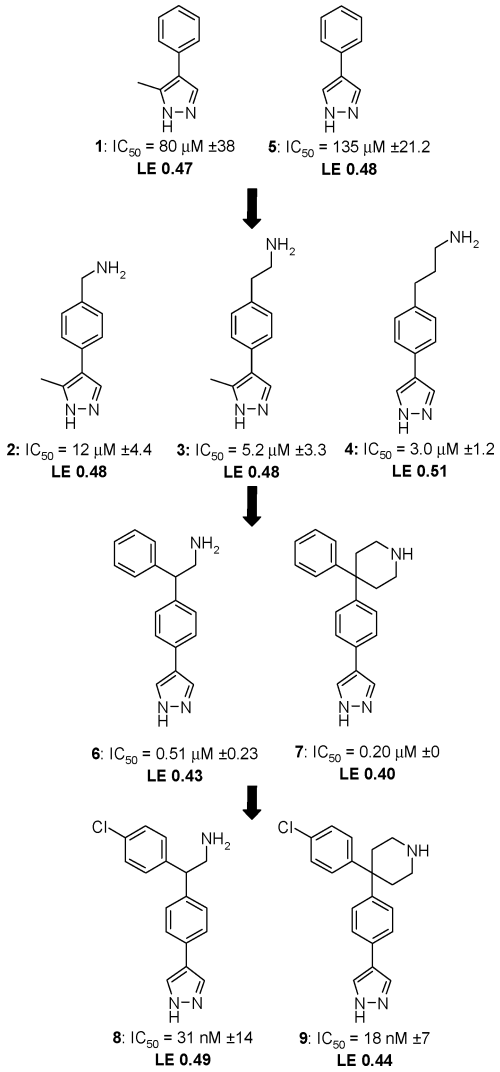

Figure 1. Progression from initial μM fragment hit **1** to nM leads **8** and **9**. Inhibition of PKBβ kinase activity determined in a radiometric filter binding assay. IC_{50} quoted is the mean value (±SEM) for at least $n = 3$ determinations. The literature compound, H-8 gave $IC_{50} = 7.5$ μM (±2.5) in this assay.[12] Compound **8** was later resolved to provide the (*R*)-enantiomer **8a** (34 nM ±11) and the (*S*)-enantiomer **8b** (0.28 μM ±0.03).

Herein we describe the application of X-ray crystallography for the rapid development of a potent series of ATP competitive inhibitors of PKB. Fragment screening[14,15] was carried out using our "Pyramid" approach, which has been described previously and applied to a number of therapeutic targets, including kinases.[16,17] This approach identified fragment **1** as an X-ray hit when it was soaked into crystals of PKA−PKB (see Figure 1). The fragment binds to the hinge region of the kinase via hydrogen bonds with the backbone N−H of Ala123 and backbone carbonyl of Glu121 (Figure 2a). Though only moderately potent, fragment **1** demonstrates a high degree of ligand efficiency and, as such, was considered to represent a useful start point for further optimization using a fragment growing strategy. Ligand efficiency (LE) has been defined by Hopkins et al.[18] as $LE = -\Delta G/HAC$, where ΔG is the free

† Coordinates and structure factors for the protein−ligand complexes have been deposited in the PDB with the following accession codes: 2uw3 (PKA-PKB-**1**), 2uw4 (PKA-PKB-**3**), 2uw5 (PKA-PKB-**8**), 2uw6 (PKA-PKB-**8b**), 2uw7 (PKA-PKB-**9**), 2uw9 (PKBβ-**9**), and 2uw8 (PKA-PKB-**10**).

* To whom correspondence should be addressed. Phone: +44 1223 226269. Fax: +44 1223 226201. E-mail: s.woodhead@astex-therapeutics.com.

‡ Astex Therapeutics Ltd.

§ Institute of Cancer Research, Chester Beatty Laboratories.

|| Cancer Research UK Centre for Cancer Therapeutics

[a] Abbreviations: PKB, protein kinase B; PKA, protein kinase A; LE, ligand efficiency; HAC, heavy atom count; GE, group efficiency.

10.1021/jm070091b CCC: $37.00
Published on Web 04/24/2007

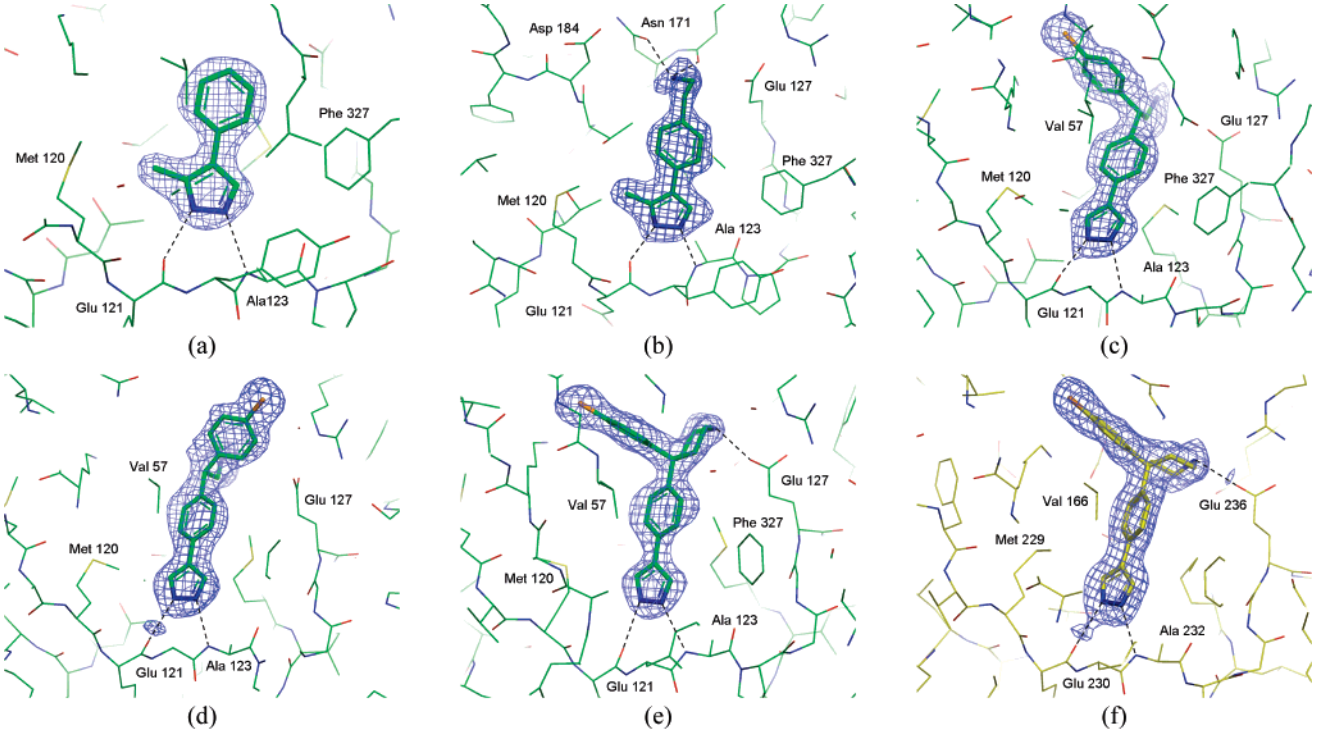

Figure 2. X-ray structures of key inhibitors bound to PKA−PKB and PKBβ in the region of the ATP site. (a) PKA−PKB−**1**, (b) PKA−PKB−**3**, (c) PKA−PKB−**8**, (d) PKA−PKB−**8b**, (e) PKA−PKB−**9**, and (f) PKBβ−**9**. The final ligand $2mF_o - DF_c$ map (contoured at 1σ) is shown in blue. Hydrogen bonds are denoted by dashed lines.

energy of binding of a compound, which can be estimated from its IC_{50}, and HAC is the number of nonhydrogen atoms in the compound (see also Kuntz et al.[19]). Monitoring and maintaining ligand efficiency during design cycles is considered important to ensure that the final compound exhibits desirable physicochemical properties. To obtain a final compound with MW < 500 Da and ~10 nM potency, ligand efficiency needs to stay above 0.30 kcal/mol per heavy atom.

Inspection of the 3D structure of fragment **1** suggested that a basic group could be added to probe the ribose binding pocket, an electronegative region of the protein formed by residues Glu127, Glu170, Asn171, and Asp184. Accordingly, we synthesized compounds **2**−**4** (Figure 1). Bioassay data demonstrated that attaching a basic amine can result in up to 30-fold improvement in the potency of these compounds while retaining the ligand efficiency of the initial fragment. The X-ray structure of compound **3** (Figure 2b) confirmed the expected interactions between the basic amine and residues in the electronegative pocket. In addition, we tested compound **5**, the des-methyl analog of fragment **1**, and found that the methyl group only provided a marginal improvement to the potency. In the next design cycle, aromatic rings were incorporated into the compounds to access a lipophilic pocket adjacent to the glycine rich loop. Two of these compounds, **6** and **7**, are shown in Figure 1. The addition of the phenyl ring results in a 10-fold improvement in potency and sub-μM affinity for PKBβ, with only limited loss of ligand efficiency. A further improvement in potency is obtained by incorporating a chloro substituent in the 4-position of the phenyl ring, as is shown for compounds **8** and **9** in Figure 1. Again, a 10-fold improvement in potency is achieved, and the high ligand efficiency of the compounds is maintained. The X-ray structures of compounds **8** and **9** (Figure 2c,e) reveal that the chlorophenyl group forms hydrophobic contacts with the lipophilic pocket as expected.

In the crystal structure of racemic **8** with PKA−PKB, only the (*R*)-enantiomer **8a** was observed. Chromatographic resolution of **8** subsequently confirmed that the (*R*)-enantiomer **8a** was 10-fold more active than the (*S*)-enantiomer **8b** and the binding mode of **8a** was identical to that observed for the racemate. The protein−ligand structure of the (*S*)-enantiomer **8b**, while maintaining the interactions with the hinge region, does not occupy the lipophilic pocket. Instead, the chlorophenyl is directed toward the side chain of Tyr330 (see Figure 2d). The analogous 4-chloro-substituted compound **9** adopts a similar binding mode in PKA−PKB to that observed for **8a**, but has the advantage of being achiral. As a final confirmation step, we determined the protein−ligand structure of **9** with PKBβ (see Figure 2f). Although there are subtle changes in the conformation of the piperidine ring, the inhibitor adopts essentially the same binding mode in both PKA−PKB and PKBβ. The gross binding mode of **9** is comparable to that of a related 6-phenylpurine discovered through parallel optimization of an azaindole fragment hit.[20]

A Free−Wilson analysis[21] of the SAR data in Figure 3 allowed us to estimate how the potency of compound **8a** is distributed throughout the molecule. Group contributions to the free energy, d*G*, for the various parts of the compound are also listed in this figure. It is inappropriate to directly use the potency of the simple heterocycle pyrazole as the d*G* of the pyrazole group in compound **8a**. This is because the free energy of binding of the compound also contains the free energy associated with the loss of rigid body entropy on binding to the enzyme, that is, $\Delta G = \Delta G_{int} + \Delta G_{rigid}$. In this equation, ΔG_{int} is the *intrinsic* binding affinity of the compound and includes favorable terms (such as hydrogen bonds) and unfavorable terms (such as freezing rotatable bonds) and ΔG_{rigid} is the free energy associated with the loss of rigid body entropy on binding to the enzyme. We have shown in a recent study that this penalty can be considerable: approximately 4.2 kcal/mol, that is, about 2−3 orders of magnitude in potency.[22] To bring the pyrazole contribution onto the same scale as the other d*G* terms in Figure

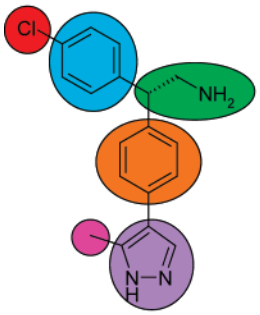

Compound	Pyr	Me[a)]	Phe1	EtNH$_2$	Phe2	Cl	ΔG
1	✓	✓	✓				-6.0
3	✓	✓	✓	✓			-7.6
5	✓		✓				-5.7
6	✓		✓	✓	✓		-9.0
8a	✓		✓	✓	✓	✓	-10.6
pyrazole	✓						-3.1[b)]
dG	-7.3[c)]	-0.32	-2.5	-1.6	-1.7	-1.6	
GE	1.5	0.32	0.42	0.54	0.28	1.6	

a) This methyl group is not present in compound **8a**, but is needed for the Free Wilson analysis.
b) Pyrazole inhibited PKB too weakly to determine an IC_{50} in the bioassay. The value presented is an estimate based on crystallographic assessment of changes in the occupancy of pyrazole (in PKA-PKB) with varying compound concentration.
c) Calculated as $dG=\Delta G-\Delta G_{rigid}$, using $\Delta G_{rigid}=4.2$kcal/mol.

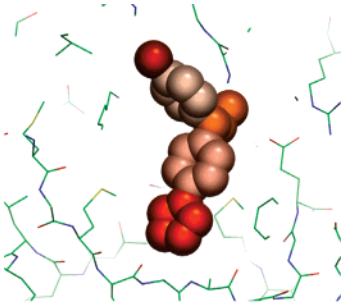

Figure 3. Free−Wilson analysis of the SAR around compound **8a**, resulting group contributions d*G* and group efficiencies, GE. The different functional groups are defined according to the color scheme provided on the left. On the right, the binding mode of compound **8a** is shown, with the atoms of the compound color coded according to their group efficiencies.

3, this rigid-body barrier to binding was, therefore, subtracted from the free energy of binding of pyrazole.

This simple analysis reveals that the majority of the intrinsic binding affinity of compound **8a** resides in the pyrazole. This finding is consistent with observations that the potency of a compound is often unevenly distributed throughout the molecule and in many cases concentrated in an "anchor fragment".[23] The d*G* values can be converted into "group efficiencies" (GE), which are defined analogously to ligand efficiencies as GE = −d*G*/HAC, where HAC is the number of nonhydrogen atoms in a particular group. Again, to stay within drug-like space, an approximate guideline of GE ≥ 0.3 is used. The group efficiencies highlight the fact that the 4-chloro substituent on the terminal phenyl ring has been a particularly efficient addition. Analyses like these can be useful to prioritize compounds and to assess which regions of the binding site should be explored to optimize potency.[24] Figure 3 also shows the X-ray binding mode of compound **8a** color-coded according to the GE values of the functional groups.

Subsequently, we discovered that compound **10** (Figure 4) still has a reasonable potency (77 μM) and acceptable ligand efficiency, even though it lacks the pyrazole that forms the key interactions with the hinge region. The (*R*)-enantiomer of **10** adopts a similar binding mode to the fully elaborated compounds, with the chlorophenyl occupying the lipophilic pocket. However, there is some disorder in the structure of **10** and evidence for a small population of chlorophenyl binding toward the hinge. This could be interpreted both as binding of the (*S*)-enantiomer of **10** (which was present as the racemate) and/or an alternate binding mode of the (*R*)-enantiomer.

Compound **8a** is essentially a combination of compounds **10** and pyrazole. It is interesting to retrospectively assess how

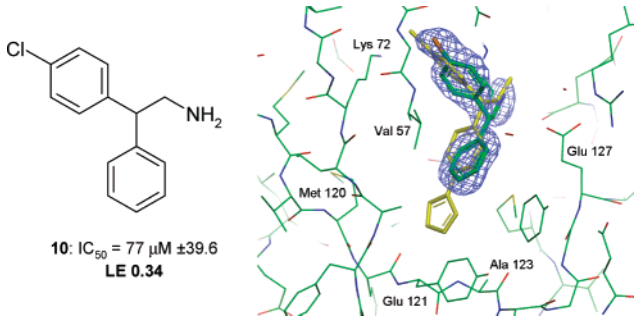

Figure 4. X-ray structure of compound **10** bound to PKA−PKB. The final ligand $2mF_o - DF_c$ map (contoured at 1σ) is shown in blue. For comparison, the binding mode of compound **8a** was superimposed and is shown in yellow. IC_{50} quoted is the mean value (±SEM) for at least $n = 3$ determinations.

efficiently the "linking" of these two fragments was done had this been a fragment-linking exercise. If two fragments are linked, superadditivity of their potencies may be observed, as the combined compound only pays the rigid-body penalty to binding once, whereas the fragments each have to overcome this barrier individually. When two fragments are linked ideally, the combined compound can be 2−3 orders of magnitude more potent than would be expected based on the potencies of the individual fragments.[22] Simply adding the free energies of binding of compounds **10** and pyrazole gives −9.0 kcal/mol. The actual free energy of binding of compound **8a** is −10.8 kcal/mol, implying that superadditivity was indeed achieved and that the fragments were "linked" efficiently. Nevertheless, the extra −1.8 kcal/mol gained by linking the two compounds is less than might be expected when two fragments are linked ideally. There are several factors that could have contributed to this: (i) compound **10** shows some disorder in the X-ray structure (see above) and this could have increased the potency of compound **10**; (ii) an extra rotational bond has been introduced by linking the compounds, which is frozen out when compound **8a** binds to the protein; (iii) linking the two fragments could have affected the electronics of the ring systems and hence their interaction with the protein; and (iv) the overlay of compounds **8a** with **10** is imperfect (see Figure 4), linking **10** to the pyrazole shifts it higher up in the pocket, inevitably losing some of this potency.

In summary, fragment-based drug discovery using our Pyramid platform has facilitated the rapid identification of novel, low molecular weight (<350 Da) PKB/Akt inhibitors. By applying protein−ligand crystallography to iterative structure-based design we have successfully elaborated an initial fragment hit **1** into nanomolar PKBβ inhibitors **8a** and **9**. In addition, by using a Free−Wilson analysis, we have been able to estimate the binding efficiency of the individual functional groups in compound **8a**, with a view to directing further optimization.

Acknowledgment. The authors acknowledge Susanne Saalau-Bethell and Brent Graham for protein purification, Wendy Blakemore for crystallographic support, Lisa Seavers and Deborah Davis for IC_{50} determinations, and Cesare Granata for HPLC purifications.

Supporting Information Available: Experimental procedures for the preparation of compounds **8** and **9**, HPLC conditions for the chiral resolution of compound **8**, and X-ray crystallography statistics. This material is available free of charge via the Internet at http://pubs.acs.org.

References

(1) Brazil, D. P.; Yang, Z. Z.; Hemmings, B. A. Advances in protein kinase B signalling: AKTion on multiple fronts. *Trends Biochem. Sci.* **2004**, *29*, 233−242.

(2) Hill, M. M.; Hemmings, B. A. Inhibition of protein kinase B/Akt. Implications for cancer therapy. *Pharmacol. Ther.* **2002**, *93*, 243−251.

(3) Barnett, S. F.; Bilodeau, M. T.; Lindsley, C. W. The Akt/PKB family of protein kinases: A review of small molecule inhibitors and progress towards target validation. *Curr. Top. Med. Chem.* **2005**, *5*, 109−125.

(4) Li, Q.; Zhu, G. D. Targeting serine/threonine protein kinase B/Akt and cell-cycle checkpoint kinases for treating cancer. *Curr. Top. Med. Chem.* **2002**, *2*, 939−971.

(5) Vivanco, I.; Sawyers, C. L. The phosphatidylinositol 3-kinase AKT pathway in human cancer. *Nat. Rev. Cancer* **2002**, *2*, 489−501.

(6) Yang, L.; Dan, H. C.; Sun, M.; Liu, Q.; Sun, X. m.; Feldman, R. I.; Hamilton, A. D.; Polokoff, M.; Nicosia, S. V.; Herlyn, M.; Sebti, S. M.; Cheng, J. Q. Akt/protein kinase B signaling inhibitor-2, a selective small molecule inhibitor of Akt signaling with antitumor activity in cancer cells overexpressing Akt. *Cancer Res.* **2004**, *64*, 4394−4399.

(7) Breitenlechner, C. B.; Friebe, W. G.; Brunet, E.; Werner, G.; Graul, K.; Thomas, U.; Kunkele, K. P.; Schafer, W.; Gassel, M.; Bossemeyer, D.; Huber, R.; Engh, R. A.; Masjost, B. Design and crystal structures of protein kinase B-selective inhibitors in complex with protein kinase A and mutants. *J. Med. Chem.* **2005**, *48*, 163−170.

(8) Lin, X.; Murray, J. M.; Rico, A. C.; Wang, M. X.; Chu, D. T.; Zhou, Y.; Del Rosario, M.; Kaufman, S.; Ma, S.; Fang, E.; Crawford, K.; Jefferson, A. B. Discovery of 2-pyrimidyl-5-amidothiophenes as potent inhibitors for AKT: Synthesis and SAR studies. *Bioorg. Med. Chem Lett.* **2006**, *16*, 4163−4168.

(9) Woods, K. W.; Fischer, J. P.; Claiborne, A.; Li, T.; Thomas, S. A.; Zhu, G. D.; Diebold, R. B.; Liu, X.; Shi, Y.; Klinghofer, V.; Han, E. K.; Guan, R.; Magnone, S. R.; Johnson, E. F.; Bouska, J. J.; Olson, A. M.; de Jong, R.; Oltersdorf, T.; Luo, Y.; Rosenberg, S. H.; Giranda, V. L.; Li, Q. Synthesis and SAR of indazole−pyridine based protein kinase B/Akt inhibitors. *Bioorg. Med. Chem* **2006**, *14*, 6832−6846.

(10) Yang, J.; Cron, P.; Good, V. M.; Thompson, V.; Hemmings, B. A.; Barford, D. Crystal structure of an activated Akt/protein kinase B ternary complex with GSK3−peptide and AMP−PNP. *Nat. Struct. Biol.* **2002**, *9*, 940−944.

(11) Luo, Y.; Shoemaker, A. R.; Liu, X.; Woods, K. W.; Thomas, S. A.; De Jong, R.; Han, E. K.; Li, T.; Stoll, V. S.; Powlas, J. A.; Oleksijew, A.; Mitten, M. J.; Shi, Y.; Guan, R.; McGonigal, T. P.; Klinghofer, V.; Johnson, E. F.; Leverson, J. D.; Bouska, J. J.; Mamo, M.; Smith, R. A.; Gramling-Evans, E. E.; Zinker, B. A.; Mika, A. K.; Nguyen, P. T.; Oltersdorf, T.; Rosenberg, S. H.; Li, Q.; Giranda, V. L. Potent and selective inhibitors of Akt kinases slow the progress of tumors in vivo. *Mol. Cancer Ther.* **2005**, *4*, 977−986.

(12) Collins, I.; Caldwell, J.; Fonseca, T.; Donald, A.; Bavetsias, V.; Hunter, L. J.; Garrett, M. D.; Rowlands, M. G.; Aherne, G. W.; Davies, T. G.; Berdini, V.; Woodhead, S. J.; Davis, D.; Seavers, L. C.; Wyatt, P. G.; Workman, P.; McDonald, E. Structure-based design of isoquinoline-5-sulfonamide inhibitors of protein kinase B. *Bioorg. Med. Chem.* **2006**, *14*, 1255−1273.

(13) Davies, T. G.; Verdonk, M. L.; Graham, B.; Saalau-Bethell, S.; Hamlett, C. C.; McHardy, T.; Collins, I.; Garrett, M. D.; Workman, P.; Woodhead, S. J.; Jhoti, H.; Barford, D. A structural comparison of inhibitor binding to PKB, PKA, and PKA−PKB chimera. *J. Mol. Biol.* **2007**, *367*, 882−894.

(14) Rees, D. C.; Congreve, M.; Murray, C. W.; Carr, R. Fragment-based lead discovery. *Nat. Rev. Drug Discovery* **2004**, *3*, 660−672.

(15) Erlanson, D. A.; McDowell, R. S.; O'Brien, T. Fragment-based drug discovery. *J. Med. Chem.* **2004**, *47*, 3463−3482.

(16) Hartshorn, M. J.; Murray, C. W.; Cleasby, A.; Frederickson, M.; Tickle, I. J.; Jhoti, H. Fragment-based lead discovery using X-ray crystallography. *J. Med. Chem* **2005**, *48*, 403−413.

(17) Mooij, W. T.; Hartshorn, M. J.; Tickle, I. J.; Sharff, A. J.; Verdonk, M. L.; Jhoti, H. Automated protein−ligand crystallography for structure-based drug design. *ChemMedChem* **2006**, *1*, 827−838.

(18) Hopkins, A. L.; Groom, C. R.; Alex, A. Ligand efficiency: A useful metric for lead selection. *Drug Discovery Today* **2004**, *9*, 430−431.

(19) Kuntz, I. D.; Chen, K.; Sharp, K. A.; Kollman, P. A. The maximal affinity of ligands. *Proc. Natl. Acad. Sci. U.S.A.* **1999**, *96*, 9997−10002.

(20) Donald, A.; McHardy, T.; Rowlands, M. G.; Hunter, L.-J. K.; Davies, T. G.; Berdini, V.; Boyle, R. G.; Aherne, G. W.; Garrett, M. D.; Collins, I. Rapid evolution of 6-phenylpurine inhibitors of protein kinase B through structure-based design. *J. Med. Chem.* **2007**, *50*, 2289−2292.

(21) Free, S. M.; Wilson, J. W. A mathematical contribution to structure−activity studies. *J. Med. Chem.* **1964**, *7*, 395−399.

(22) Murray, C. W.; Verdonk, M. L. The consequences of translational and rotational entropy lost by small molecules on binding to proteins. *J. Comput.-Aided Mol. Des* **2002**, *16*, 741−753.

(23) Rejto, P. A.; Verkhivker, G. M. Unraveling principles of lead discovery: From unfrustrated energy landscapes to novel molecular anchors. *Proc. Natl. Acad. Sci. U.S.A* **1996**, *93*, 8945−8950.

(24) Ciulli, A.; Williams, G.; Smith, A. G.; Blundell, T. L.; Abell, C. Probing hot spots at protein−ligand binding sites: A fragment-based approach using biophysical methods. *J. Med. Chem.* **2006**, *49*, 4992−5000.

JM070091B